

Quark models of dibaryon resonances in nucleon-nucleon scattering

J.L. Ping¹, H.X. Huang¹, H.R. Pang², Fan Wang³ and C.W. Wong⁴

¹*Department of Physics, Nanjing Normal University, Nanjing, 210097, P.R. China*

²*Department of Physics, Southeast University, Nanjing, 210094, P.R. China*

³*Department of Physics, Nanjing University, Nanjing, 210093, P.R. China*

⁴*Department of Physics and Astronomy, University of California, Los Angeles, CA 90095-1547, USA*

We look for $\Delta\Delta$ and $N\Delta$ resonances by calculating NN scattering phase shifts of two interacting baryon clusters of quarks with explicit coupling to these dibaryon channels. Two phenomenological nonrelativistic chiral quark models giving similar low-energy NN properties are found to give significantly different dibaryon resonance structures. In the chiral quark model (ChQM), the dibaryon system does not resonate in the NN S -waves, in agreement with the experimental SP07 NN partial-wave scattering amplitudes. In the quark delocalization and color screening model (QDCSM), the S -wave NN resonances disappear when the nucleon size b falls below 0.53 fm. Both quark models give an $IJ^P = 03^+$ $\Delta\Delta$ resonance. At $b = 0.52$ fm, the value favored by baryon spectrum, the resonance mass is 2390 (2420) MeV for the ChQM with quadratic (linear) confinement, and 2360 MeV for the QDCSM. Accessible from the ${}^3D_3^{NN}$ channel, this resonance is a promising candidate for the known isoscalar ABC structure seen more clearly in the $pn \rightarrow d\pi\pi$ production cross section at 2410 MeV in the recent preliminary data reported by the CELSIUS-WASA Collaboration. In the isovector dibaryon sector, our quark models give a bound or almost bound ${}^5S_2^{\Delta\Delta}$ state that can give rise to a ${}^1D_2^{NN}$ resonance. None of the quark models used has bound $N\Delta$ P -states that might generate odd-parity resonances.

PACS numbers: 12.39.Jh, 14.20.Pt, 13.75.Cs

I. INTRODUCTION

Quantum chromodynamics (QCD) is widely accepted as the fundamental theory of the strong interaction. Lattice QCD methods have recently been used to study low-energy hadronic interactions, including the nucleon-nucleon (NN) interaction [1]. However, QCD-inspired quark models are still the main tool for detailed studies of the baryon-baryon interaction.

The phenomenological quark model most commonly used in the study of NN interaction is the nonrelativistic chiral quark model (ChQM) [2, 3, 4]. Nonrelativistic kinematics makes the many-body treatment of the multi-quark system manageable, with the very convenient choice that the light quark mass m_q is just one third of the nucleon mass. With quarks, one needs a confinement potential to reproduce a distinctive QCD property, and a one gluon exchange (OGE) to account for Δ - N mass difference and other details of baryon excitations. The inclusion of pion exchange will take care of long-range baryon-baryon interactions as well as some features in baryon structure, and is the consequence of the relative weakness of chiral symmetry breaking. Finally, scalar exchange is used to describe an extra intermediate-range attraction needed in nuclear forces. No other meson exchanges are included. ChQMs with a few chosen and a few adjusted parameters are able to give a surprisingly simple if only semi-quantitative picture of both baryon spectra and baryon-baryon interactions at relatively low energies. It is therefore of some interest to understand some of the limitations of these simple quarks models.

The most problematic term in the ChQM is the scalar exchange term. It takes into account neglected chan-

nels containing Δ s and pions, and should therefore vary when more of these channels are explicitly included in the coupled-channel calculation. Its effects always include the exchange of two pions, and are called correlated if the two pions also interact with each other. Modern treatments of correlated two-pion exchange show that in addition to a long-range scalar-isoscalar attraction traditionally associated with scalar exchange, there is also a strong scalar-isoscalar repulsive core [5], a complication that has not yet been included in the ChQM.

In the quark model, the forces between baryonic clusters of quarks and antiquarks are like molecular forces between molecules of atoms built up from the forces between their constituents. This molecular model of nuclear forces has been extensively developed by using the quark delocalization and color screening model (QDCSM) [6]. In this model, quarks confined in one baryon are allowed to delocalize to a nearby baryon and to change the dynamics of the baryon-baryon interaction through a reduction of the confinement potential called color screening. The delocalization parameter that appears is determined by the dynamics of the interacting quark system, thus making it possible for the quark system to reach a more favorable configuration through its own dynamics in a larger Hilbert space. The model has been successfully applied to NN and hyperon-nucleon scatterings. The important intermediate-range NN attraction is achieved in this model by the mutual distortion of the interacting nucleons, in a way that is very similar to the mutual distortion of interacting molecules.

The main difference between the ChQM and the QDCSM is the mechanism for intermediate-range attraction. Recently, we showed that both the ChQM containing the

σ -meson and the QDCSM without it gave a good description of the low-energy NN S - and D -wave scattering phase shifts and the properties of deuteron with almost the same quark-model parameters [7]. Thus the σ -meson exchange can effectively be replaced by the quark delocalization and color screening mechanism. It is not clear however if their equivalence persists to higher energies where nucleons overlap more strongly and baryon excitation and multiquark effects become more important.

Interest in multiquark system has persisted since R. Jaffe predicted the H-particle in 1977 [8]. All quark models, including those using lattice QCD techniques, predict that in addition to the $q\bar{q}$ mesons and q^3 baryons, there should be multiquark systems $(q\bar{q})^2$, $q^4\bar{q}$, q^6 , quark gluon hybrids $qq\bar{q}g$, q^3g , and glueballs [9]. Up to now there has been no well established experimental candidate of these multiquark states [10]. Recently, the CELSIUS-WASA Collaboration has reported preliminary results on the ABC anomaly in the production cross section of the $pn \rightarrow d\pi^0\pi^0$ reaction that suggests the presence of an isoscalar $J^P = 1^+$ or 3^+ subthreshold $\Delta\Delta$ resonance, with resonance mass estimated at ~ 2410 MeV and a width of < 100 MeV [11]. The relatively large binding energy involved gives an object that is much closer to these interesting multiquark states than a loosely bound system like the deuteron. Nonrelativistic quark models such as ChQMs and QDCSMs fitting both N, Δ masses and low-energy NN scattering properties can be expected to give particularly interesting and parameter-free predictions for such dibaryon multiquark states.

It thus appears worthwhile to extend our past calculation of NN phase shifts to the resonance region near the $\Delta\Delta$ and $N\Delta$ thresholds by including these excited dibaryon channels in coupled-channel calculations. The Δ resonance is by far the most important low-energy baryon resonance. It dominates even the π^-p cross sections where its production is hindered relative to the production of isospin $1/2$ N^* resonances by a factor of 2 from isospin coupling. In dibaryon channels, the $\Delta\Delta$ threshold at 2460 MeV is clearly separated from the $NN^*(1440)$ threshold at 2380 MeV, the second most interesting dibaryon threshold in this energy region. $\Delta\Delta$ bound states are of immediate interest in understanding resonance phenomena in this near subthreshold energy region. The inclusion of $N^*(1440)$ would be of considerable interest in a broader study of dibaryon resonances, but its inclusion is technically difficult for us because $N^*(1440)$ is commonly understood to be a monopole excitation of the nucleon that has a much more complicated quark wave function. In contrast, our approximate description of the $N \rightarrow \Delta$ excitation as a simple spin-isospin excitation without any change in the radial wave function probably captures the essence of the physics involved. Δ excitations are thus within easy reach of the technology used in our previous coupled-channel calculations.

Our first study in the resonance region will include only Δ excitations. This limitation of excited baryon degrees of freedom to Δ s only has often been made in past studies of nuclear forces. [12]

We shall use the same Salamanca ChQM [13] and QDCSM used previously for NN channels only [7] with additional sets of potential parameters to find out if their similarity persists into the resonance region. We are interested in particular in discovering how similar these simple quark models are in describing theoretical dibaryon resonances originating from $\Delta\Delta$ or $N\Delta$ bound states when the Δ s are treated as stable particles. In other words, these dibaryon resonances are theoretical compound dibaryon states that are allowed to decay only via the NN channels. A brief description of these two quark models of the baryon-baryon interaction is given in Section II.

The NN phase shifts for these quark-quark potentials are calculated using a coupled-channel resonating group formalism [14] that includes $\Delta\Delta$, $N\Delta$ and sometimes hidden-color channels as well. No explicit pionic channels are included as the Δ s are treated as stable particles. In this context, a promising dibaryon resonance is taken to be one arising from a bound state below the $\Delta\Delta$ or $N\Delta$ threshold. The calculated results, including resonance masses and widths (FWHMs), are given in section III in those partial waves (PWs) where a theoretical dibaryon resonance appears in at least one quark model. No $N\Delta$ bound state is found in any isovector odd-parity state in all our quark models.

In Sect. IV, these results are compared to partial-wave analyses of NN scattering amplitudes [15, 16], where the presence of a dibaryon resonance causes a rapid counterclockwise motion in the Argand diagram. The possibility that the ABC effect in the $pn \rightarrow d\pi\pi$ reaction is an isoscalar NN resonance is also discussed.

Section V contains brief concluding remarks on what we have learned about quark dynamics in the NN resonance region.

II. TWO QUARK MODELS OF BARYON-BARYON INTERACTIONS

A. Chiral quark model

The Salamanca ChQM is representative of chiral quark models. It has also been used to describe both hadron spectroscopy and nucleon-nucleon interactions. The model details can be found in [13]. Only the Hamiltonian and parameters are given here.

The ChQM Hamiltonian in the baryon-baryon sector is

$$\begin{aligned}
H &= \sum_{i=1}^6 \left(m_i + \frac{p_i^2}{2m_i} \right) - T_c + \sum_{i<j} [V^G(r_{ij}) + V^\pi(r_{ij}) + V^\sigma(r_{ij}) + V^\rho(r_{ij}) + V^C(r_{ij})], \quad (1) \\
V^G(r_{ij}) &= \frac{1}{4} \alpha_s \boldsymbol{\lambda}_i \cdot \boldsymbol{\lambda}_j \left[\frac{1}{r_{ij}} - \frac{\pi}{m_q^2} \left(1 + \frac{2}{3} \boldsymbol{\sigma}_i \cdot \boldsymbol{\sigma}_j \right) \delta(r_{ij}) - \frac{3}{4m_q^2 r_{ij}^3} S_{ij} \right] + V_{ij}^{G,LS}, \\
V_{ij}^{G,LS} &= -\frac{\alpha_s}{4} \boldsymbol{\lambda}_i \cdot \boldsymbol{\lambda}_j \frac{1}{8m_q^2 r_{ij}^3} [\mathbf{r}_{ij} \times (\mathbf{p}_i - \mathbf{p}_j)] \cdot (\boldsymbol{\sigma}_i + \boldsymbol{\sigma}_j), \\
V^\pi(r_{ij}) &= \frac{1}{3} \alpha_{ch} \frac{\Lambda^2}{\Lambda^2 - m_\pi^2} m_\pi \left\{ \left[Y(m_\pi r_{ij}) - \frac{\Lambda^3}{m_\pi^3} Y(\Lambda r_{ij}) \right] \boldsymbol{\sigma}_i \cdot \boldsymbol{\sigma}_j + \left[H(m_\pi r_{ij}) - \frac{\Lambda^3}{m_\pi^3} H(\Lambda r_{ij}) \right] S_{ij} \right\} \boldsymbol{\tau}_i \cdot \boldsymbol{\tau}_j, \\
V^\sigma(r_{ij}) &= -\alpha_{ch} \frac{4m_u^2}{m_\pi^2} \frac{\Lambda^2}{\Lambda^2 - m_\sigma^2} m_\sigma \left[Y(m_\sigma r_{ij}) - \frac{\Lambda}{m_\sigma} Y(\Lambda r_{ij}) \right] + V_{ij}^{\sigma,LS}, \quad \alpha_{ch} = \frac{g_{ch}^2}{4\pi} \frac{m_\pi^2}{4m_u^2}, \\
V_{ij}^{\sigma,LS} &= -\frac{\alpha_{ch}}{2m_\pi^2} \frac{\Lambda^2}{\Lambda^2 - m_\sigma^2} m_\sigma^3 \left[G(m_\sigma r_{ij}) - \frac{\Lambda^3}{m_\sigma^3} G(\Lambda r_{ij}) \right] [\mathbf{r}_{ij} \times (\mathbf{p}_i - \mathbf{p}_j)] \cdot (\boldsymbol{\sigma}_i + \boldsymbol{\sigma}_j), \\
V^\rho(r_{ij}) &= \alpha_{chw} \frac{4m_u^2}{m_\pi^2} \frac{\Lambda^2}{\Lambda^2 - m_\rho^2} m_\rho \left\{ \left[Y(m_\rho r_{ij}) - \frac{\Lambda}{m_\rho} Y(\Lambda r_{ij}) \right] + \frac{m_\rho^2}{6m_u^2} \left[Y(m_\rho r_{ij}) - \frac{\Lambda^3}{m_\rho^3} Y(\Lambda r_{ij}) \right] \boldsymbol{\sigma}_i \cdot \boldsymbol{\sigma}_j \right. \\
&\quad \left. - \frac{1}{2} \left[H(m_\rho r_{ij}) - \frac{\Lambda^3}{m_\rho^3} H(\Lambda r_{ij}) \right] S_{ij} \right\} \boldsymbol{\tau}_i \cdot \boldsymbol{\tau}_j + V_{ij}^{\rho,LS}, \quad \alpha_{chw} = \frac{g_{chw}^2}{4\pi} \frac{m_\pi^2}{4m_u^2}, \\
V_{ij}^{\rho,LS} &= -\frac{3\alpha_{chw}}{m_\pi^2} \frac{\Lambda^2}{\Lambda^2 - m_\rho^2} m_\rho^3 \left[G(m_\rho r_{ij}) - \frac{\Lambda^3}{m_\rho^3} G(\Lambda r_{ij}) \right] [\mathbf{r}_{ij} \times (\mathbf{p}_i - \mathbf{p}_j)] \cdot (\boldsymbol{\sigma}_i + \boldsymbol{\sigma}_j) \boldsymbol{\tau}_i \cdot \boldsymbol{\tau}_j, \\
V^C(r_{ij}) &= -a_c \boldsymbol{\lambda}_i \cdot \boldsymbol{\lambda}_j (r_{ij}^2 + V_0) + V_{ij}^{C,LS}, \\
V_{ij}^{C,LS} &= a_c \boldsymbol{\lambda}_i \cdot \boldsymbol{\lambda}_j \frac{1}{8m_q^2 r_{ij}} \frac{1}{dr_{ij}} [\mathbf{r}_{ij} \times (\mathbf{p}_i - \mathbf{p}_j)] \cdot (\boldsymbol{\sigma}_i + \boldsymbol{\sigma}_j), \quad V^c = r_{ij}^2, \\
S_{ij} &= \frac{(\boldsymbol{\sigma}_i \cdot \mathbf{r}_{ij})(\boldsymbol{\sigma}_j \cdot \mathbf{r}_{ij})}{r_{ij}^2} - \frac{1}{3} \boldsymbol{\sigma}_i \cdot \boldsymbol{\sigma}_j. \quad (2)
\end{aligned}$$

Here S_{ij} is quark tensor operator, $Y(x)$, $H(x)$ and $G(x)$ are standard Yukawa functions [17], T_c is the kinetic energy of the center of mass, α_{ch} is the chiral coupling constant, determined as usual from the π -nucleon coupling constant. An additional ρ meson exchange potential V^ρ between quarks has been added to give an improved treatment of baryon-baryon P -states. Its parameters will be specified in Sect. III. All other symbols have their usual meanings.

Table I gives the model parameters used. For each set of parameters, the nucleon size b that appears in Eq.(5) is given a pre-determined value. Two of the parameters (a_c, α_s) are fitted to Δ - N mass difference (1232 - 939 MeV) and the equilibrium condition for the nucleon mass at the chosen b . The absolute nucleon mass is controlled by a constant term V_0 in the confinement potential that does not affect the baryon-baryon interaction. In ChQM2 [18], the deuteron binding energy (2.22 MeV) is fitted by varying the combination m_σ, Λ calculated with the standard two NN coupled channels 3S_1 and 3D_1 (called 2NNcc in the following). The remaining parameters m_q, m_π and α_{ch} are fixed at chosen values. The numeral 2 in the name ChQM2 refers to its quadratic

confinement potential. The model ChQM1 [2] uses a linear confinement potential instead. The model ChQM2a differs from ChQM2 in fitting a different equilibrium nucleon size b but for simplicity m_σ, Λ are allowed to remain at the ChQM2 values. Its deuteron binding energy is reduced, but we do not consider the difference to be important in our study of dibaryon resonance properties.

Finally, Table I also gives the effective-range (ER) parameters of a 5-parameter ER formula in the NN 3S_1 (1S_0) state. The calculation uses with 5 (4) color-singlet channels denoted 5cc (4cc) and defined in the following section. The channels used include 2 NN and 3 $\Delta\Delta$ (an NN , 2 $\Delta\Delta$, and an $N\Delta$) channels. The deuteron binding energy ε_d calculated from the two ER parameters of the 5cc calculation is also given in the table. According to [19], this approximation overestimates the binding energy, but by only 0.015 MeV. So the tabulated binding energies are sufficiently accurate for this qualitative study. The same ER approximation for a 2NNcc calculation gives $\varepsilon_d \approx 1.86$ MeV for ChQM2, thus showing that the 3 $\Delta\Delta$ channels increase ε_d by about 1.5 MeV.

TABLE I: Parameters that differ in different models are given in this table. The dimension of each dimensional parameter is given within parentheses following each symbol: b (fm), a_c (MeV fm^{-2} if quadratic, but MeV fm^{-1} if linear), V_0 (fm^2) and μ (fm^{-2}). Parameters having the same value for all the quark models discussed in this paper are $m_q = 313$ MeV, $m_\pi = 138$ MeV, $\Lambda/\hbar c = 4.2 \text{ fm}^{-1}$, and $m_\sigma = 675$ (MeV) for ChMQs. The scattering length and effective range calculated for each potential are also given: a_t, r_t for the triplet state 3S_1 and a_s, r_s for the singlet state 1S_0 , all in fm. The deuteron binding energy ε_d (MeV) is calculated from the triplet effective-range parameters.

	ChQM2 (ChQM1)	ChQM2a	QDCSM0	QDCSM1	QDCSM3
b	0.518	0.60	0.48	0.518	0.60
a_c	46.938 (67.0)	12.39	85.60	56.75	18.55
V_0	-1.297	0.255	-1.299	-1.3598	-0.5279
μ			0.30	0.45	1.00
α_s	0.485	0.9955	0.3016	0.485	0.9955
α_{ch}	0.027 (0.0269)	0.027	0.027	0.027	0.027
a_t	4.52	20.8	34.9	5.94	6.03
r_t	1.56	2.24	2.27	1.75	1.67
ε_d	3.35	0.11	0.04	1.75	1.64
a_s	-170	-2.48	-2.32	-6.90	-5.41
r_s	2.17	5.42	4.48	2.63	3.56

B. Quark delocalization, color screening model

The model and its extension were discussed in detail in [6, 20]. Its Hamiltonian has the same form as Eq.(1), but used with $V^\sigma = 0$ and a different confinement potential

$$V_{ij}^{CON}(r_{ij}) = -a_c \boldsymbol{\lambda}_i \cdot \boldsymbol{\lambda}_j [f_{ij}(r_{ij}) + V_0], \quad (3)$$

where $f_{ij}(r_{ij}) = r_{ij}^2$ if quarks i, j , each in the Gaussian single-quark wave function ϕ_α of Eq. (5), are on the same side of the dibaryon, i.e., both centered at $\mathbf{S}/2$ or at $-\mathbf{S}/2$. If quarks i, j are on opposite sides of the dibaryon,

$$f_{ij}(r_{ij}) = \frac{1}{\mu} \left(1 - e^{-\mu r_{ij}^2} \right). \quad (4)$$

Quark delocalization in QDCSM is realized by assuming that the single particle orbital wave function of QDCSM as a linear combination of left and right Gaussians, the single particle orbital wave functions of the ordinary quark cluster model,

$$\begin{aligned} \psi_\alpha(\mathbf{S}, \epsilon) &= (\phi_\alpha(\mathbf{S}) + \epsilon \phi_\alpha(-\mathbf{S})) / N(\epsilon), \\ \psi_\beta(-\mathbf{S}, \epsilon) &= (\phi_\beta(-\mathbf{S}) + \epsilon \phi_\beta(\mathbf{S})) / N(\epsilon), \\ N(\epsilon) &= \sqrt{1 + \epsilon^2 + 2\epsilon e^{-S^2/4b^2}}, \\ \phi_\alpha(\mathbf{S}) &= \left(\frac{1}{\pi b^2} \right)^{3/4} e^{-\frac{1}{2b^2}(\mathbf{r}_\alpha - \mathbf{S}/2)^2} \\ \phi_\beta(-\mathbf{S}) &= \left(\frac{1}{\pi b^2} \right)^{3/4} e^{-\frac{1}{2b^2}(\mathbf{r}_\beta + \mathbf{S}/2)^2}. \end{aligned} \quad (5)$$

Quark delocalization with color screening is an approximate way of including hidden-color (h.c.) effects.

The color screening constant μ in Eq.(4) is determined by fitting deuteron properties. The parameters of the QDCSM i ($i = 1, 3$) used here are those of Set i of [7], and are given again in Table I. For QDCSM0, μ is an estimated value that has not been fine tuned to the deuteron binding energy. These models differ in the equilibrium nucleon size b .

III. RESULTS

NN scattering phase shifts are calculated for the quark models of Table I to energies beyond the $\Delta\Delta$ or $N\Delta$ threshold for different choice of coupled channels. We include channels containing one or more Δ s treated as stable particles, and channels containing hidden-color (h.c.) states. The resonating-group method (RGM), described in more details in [14], is used.

Past experience has suggested that reliable estimates of resonance masses can be made using non-decaying Δ s [2]. For the theoretical $N\Delta$ resonance d' ($IJ^P = 20^-$) at the theoretical mass 2065 MeV (and an $N\Delta$ binding energy of 106 MeV), an increase in the imaginary part of the Δ resonance energy by 10 – 15 MeV is known to increase the d' mass by only a few tenth of an MeV [21]. This result suggests that the complete neglect of the imaginary part $\Gamma/2 \approx 60$ MeV of the Δ resonance energy will underestimate the d' resonance mass by perhaps 2 MeV. If this result holds generally for other resonances at other binding energies, our estimates of the resonance masses can be expected to be good to a few MeV.

The use of coupled channels containing stable Δ s does mean that the calculated NN phase shifts do not describe inelasticities correctly. Thus they cannot be compared quantitatively to experimental phase parameters above the pion-production threshold in NN channels with strong inelasticities. For this reason, the primary emphasis of this paper is the extraction of resonance energies from phase shifts in the resonance region.

Our theoretical dibaryons are made up of two stable constituents below their breakup threshold and are therefore real resonances in the model. They have finite widths that come from the coupling to open NN channels.

A. $I=0$ states

Calculational details and results for the $IJ^P = 03^+$ states are given in Table II. The number of channels used in the theory is given by N_{ch} . The theoretical pure ${}^7S_3^{\Delta\Delta}$ binding energy is next estimated by diagonalizing the Hamiltonian matrix for this state in a generator-coordinate representation where the average baryon-baryon separation is taken to be less than 6 fm (in order to keep the matrix dimension manageably small). In this way, the pure ${}^7S_3^{\Delta\Delta}$ is found to be bound by

TABLE II: The $\Delta\Delta$ or resonance mass M and decay width Γ , in MeV, in five quark models for the $IJ^P = 03^+$ states. The channels included are one channel or 1c (${}^7S_3^{\Delta\Delta}$ only), two coupled channels or 2cc ($1c + {}^3D_3^{NN}$), 4cc ($2cc + {}^{7,3}D_3^{\Delta\Delta}$), and 10 coupled channels as described in the text. The pure ${}^7S_3^{\Delta\Delta}$ bound state mass for ChQM1 is 2456 MeV [2].

N_{ch}	ChQM2		ChQM2a		QDCSM0		QDCSM1		QDCSM3	
	M	Γ	M	Γ	M	Γ	M	Γ	M	Γ
1c	2425	-	2430	-	2413	-	2365	-	2276	-
2cc	2428	17	2433	10	2416	20	2368	20	2278	19
4cc	2413	14	2424	9	2400	14	2357	14	2273	17
10cc	2393	14			-	-	-	-	-	-
10cc'	2353	17			-	-	-	-	-	-
10cc''	2351	21			-	-	-	-	-	-

35 – 190 MeV, with the ChQM2 mass 60 MeV lower than the ChQM1 mass obtained by [2]. Coupling to the ${}^3D_3^{NN}$ channel causes this bound state to change into an elastic resonance where the phase shift, shown in Fig. 1, rises through $\pi/2$ at a resonance mass that has been shifted up by 3 MeV. The same small mass increase caused by the coupling to the NN continuum is seen in all J^P states studied here. The result shows that the mass shift is always dominated by the NN scattering states below the pure bound state mass rather than those above it.

The table next shows that on coupling to the two ${}^{7,3}D_3^{\Delta\Delta}$ channels above the pure ${}^7S_3^{\Delta\Delta}$ bound state, the resonance is pushed down in mass, as expected. The effect is not large, however, being 15 MeV in ChQM2 and 11 MeV in QDCSM1, which has the same α_s .

Both the pure ${}^7S_3^{\Delta\Delta}$ bound state and the associated ${}^3D_3^{NN}$ resonance are lower in mass in QDCSM1, by about 60 MeV, than in ChQM2. Since the QDCSMs contain h.c. effects, we must first determine how much h.c. channels contribute to this mass difference. This study is done with ten channels (or case 10cc). Besides the four baryon channels shown in Table II, they include the following six h.c. channels: four 3D_3 channels of ${}^2\Delta_8$ ${}^2\Delta_8$, 4N_8 4N_8 , 4N_8 2N_8 , 2N_8 2N_8 , the 7S_3 (4N_8 4N_8) and the 7D_3 (4N_8 4N_8). Here the baryon symbol is used only to denote the isospin so that ${}^2\Delta_8$ means the $T, S = 3/2, 1/2$ color-octet state. The table shows that these six h.c. channels lower the ChQM2 resonance mass by 20 MeV. Assuming that the QDCSMs account adequately for h.c. contributions, we see that the QDCSM1 dibaryon resonance mass is now lower than that in ChQM2 by only 36 MeV.

It is interesting that the pure ${}^7S_3^{\Delta\Delta}$ bound state masses in the ChQM2 and ChQM2a of different nucleon size b differ by only 5 MeV. In contrast, both bound state and resonance masses change by 90 MeV in the two QDCSMs with the same difference in the nucleon size b . This shows that the QDCS mechanism depends sensitively on the nucleon size. The possibility of a ${}^7S_3^{\Delta\Delta}$ bound state giving rise to a subthreshold resonance has been suggested previously [22], but the resonance masses for the present quark models are higher.

TABLE III: The $\Delta\Delta$ or resonance mass M and decay width Γ , in MeV, in five quark models for the $IJ^P = 01^+$ states. The channels included are 1c (${}^3S_1^{\Delta\Delta}$ only), 2cc ($1c + {}^3S_1^{NN}$), and 5cc ($2cc + {}^3D_1^{NN} + {}^{3,7}D_1^{\Delta\Delta}$). The pure ${}^3S_1^{\Delta\Delta}$ bound-state mass for ChQM1 is 2274 MeV [2].

N_{ch}	ChQM2		ChQM2a		QDCSM0		QDCSM1		QDCSM3	
	M	Γ	M	Γ	M	Γ	M	Γ	M	Γ
1c	2366		2344		2317		2206		2115	-
2cc	nr ^a		nr		nr		nr		2408	74
5cc	nr		nr		nr		nr		2393	70

^aNo resonance in these coupled channels.

The calculated ${}^3D_3^{NN}$ phase shifts are shown in Fig. 1. They differ noticeably between two quark models of very similar parameters that differ only in the replacement of the scalar exchange in ChQM2 by the QDCS mechanism in QDCSM1. The ChQM2 phase shifts agree better with experiment than the QDCSM1 phase shifts for $100 < E_{cm} < 400$ MeV. The situation is different in the ${}^3S_1^{NN}$ state shown in Fig. 2 where the phase shifts from these two quark models agree, as already pointed out by [7].

Dibaryon resonance masses can be quite sensitive to short-range dynamics. For example, the ChQM2 resonance mass can be forced down to the lower QDCSM1 value by artificially increasing the attractive confinement interaction involving h.c. configurations that appear only for overlapping baryons. The change can be made in two different ways: Either (1) increase the color confinement interaction strength among h.c. channels, and also that between color-singlet channels and h.c. channels (a model denoted 10cc') by an overall factor of 1.3; or (2) increase the color confinement interaction between color-singlet channels and h.c. channels only (model 10cc'') by an overall factor 1.55. Fig. 1(b) shows that the resulting ${}^3D_3^{NN}$ phase shifts change noticeably only for $E_{cm} > 350$ MeV. In other words, only these ‘‘high-energy’’ NN phase shifts are sensitive to changes in short-range dynamics when shielded by the strong centrifugal barrier in the NN D -waves. Hence these changes in the confinement interactions, artificial as they are, are not excluded by the experimental phase shifts.

The resonance widths given in Table II are FWHMs. They are quite small, and agree with one another.

Results for the $IJ^P = 01^+$ state are shown in Table III and Fig. 2. The theoretical pure ${}^3S_1^{\Delta\Delta}$ state is bound by 100 – 350 MeV, around twice the ${}^7S_3^{\Delta\Delta}$ binding energy. The coupling to the ${}^3S_1^{NN}$ channel has an unexpectedly large effect, pushing up the lowest of these bound ${}^3S_1^{\Delta\Delta}$ masses, by 293 MeV in QDCSM3, so that it becomes a resonance at 2408 MeV. This very large mass shift is caused by the presence of a lower-mass state, the deuteron, in the admixed ${}^3S_1^{NN}$ channel. Admixing three additional channels with no lower bound states pushes the resonance mass down a little to give for the 5cc treatment the mass shift

$$\Delta M \equiv M_R(5cc) - M(1c) = 278 \text{ MeV}. \quad (6)$$

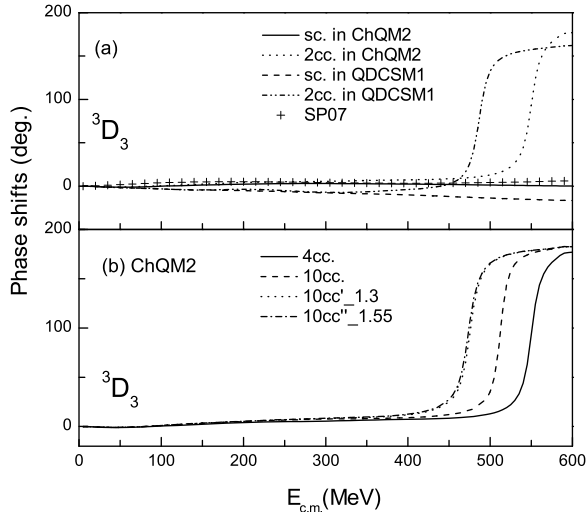


FIG. 1: (a) ${}^3D_3^{NN}$ phase shifts calculated for a single channel (sc) and two coupled channels (2cc) (${}^3D_3^{NN} + {}^7S_3^{\Delta\Delta}$) in two different quark models (ChQM2 and QDCSM1) as functions of the c.m. kinetic energy $E_{\text{cm}} = W - 2M_N$, where W is the total c.m. energy and M_N is the nucleon mass. The experimental phase shifts of the partial-wave solution SP07 [16] are also shown. (b) 3D_3 phase shifts calculated in the ChQM2 using different numbers of coupled channels, as described in more detail in the text.

The pure ${}^3S_1^{\Delta\Delta}$ bound state mass appears 100 MeV or more higher in the other four quark models. The additional large mass increase caused by the coupling to the ${}^3S_1^{NN}$ channel without or with the additional channels then pushes the state above the $\Delta\Delta$ threshold. Then no resonance appears.

The pure ${}^3S_1^{\Delta\Delta}$ bound state mass in ChQM1 is higher by 160 MeV than the QDCSM3 mass. So the ${}^3S_1^{NN}$ resonance also does not appear in ChQM1. We shall find that QDCSM3 model has an unusually rich dibaryon spectrum arising from an unusually strong attraction in $\Delta\Delta$ channels.

It is clear from Table III that the strong $\Delta\Delta$ attraction in QDCSM3 is caused by the large nucleon size b used there. As b decreases, the $\Delta\Delta$ attraction also decreases. This sensitivity to b is not seen in ChQMs, thus showing that it is caused by the QDCS mechanism.

In fact, the ${}^3S_1^{NN}$ resonance disappears somewhere between QDCSM1 and QDCSM3. The critical value b^{crit} below which the resonance disappears can be estimated under the assumption that the mass shift ΔM caused by the coupling to the ${}^3S_1^{NN}$ channels is the same for all parameter sets. The critical point then appears when the bare ${}^3S_1^{\Delta\Delta}$ bound-state mass is 2186 MeV. Interpolation from the bound-state masses shown in Table III gives $b^{\text{crit}} \approx 0.53$ fm.

In contrast, the decrease of the pure ${}^3S_1^{\Delta\Delta}$ bound state

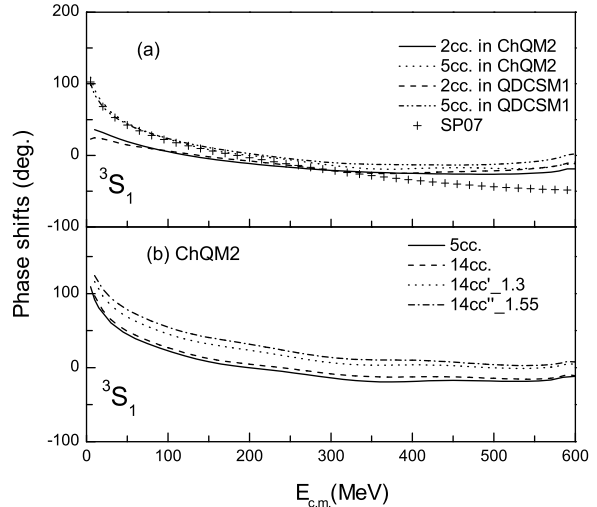


FIG. 2: (a) ${}^3S_1^{NN}$ phase shifts calculated with two or five coupled color-singlet channels defined in Table III in two different quark models ChQM2 and QDCSM1. (b) ${}^3S_1^{NN}$ phase shifts calculated in the ChQM2 using different numbers of coupled channels, as described in more detail in the text.

mass for ChQM2s as b increases from 0.52 fm to 0.60 fm is only 20% that of QDCSMs. Furthermore, b can be increased to only 0.645 fm, for the confinement potential strength a_c turns negative above that value and hence no ChQM2s can be constructed. At $b = 0.645$ fm, the pure ${}^3S_1^{\Delta\Delta}$ bound state mass is 2332 MeV, which is too large for the system to resonate on coupling to ${}^3S_1^{NN}$ channels. Hence ChQM2s have no ${}^3S_1^{NN}$ resonance.

The pure ${}^3S_1^{\Delta\Delta}$ bound state mass for ChQM1 is 2274 MeV, 92 MeV below the ChQM2 mass. If its b dependence is the same as ChQM2s, the decrease in bound state mass is insufficient, by about 50 MeV, to induce a resonance.

Turning now to the ${}^3S_1^{NN}$ phase shifts, Fig. 2 shows that ChQM2 and QDCSM1 give quite similar results, with the 5cc treatment giving much more attraction in both quark models, especially for $E_{\text{cm}} < 150$ MeV. There is fair agreement with experiment for $E_{\text{cm}} < 150$ MeV, but all theoretical phase shifts become increasingly too attractive at higher energies.

Fig. 2(b) shows the 14-channel ${}^3S_1^{NN}$ phase shifts calculated in ChQM2 with the addition of nine h.c. channels: eight ${}^3(S, D)_1$ channels of ${}^2\Delta_8^2\Delta_8$, ${}^4N_8^4N_8$, ${}^4N_8^2N_8$, ${}^2N_8^2N_8$, and ${}^7D_1^4N_8^4N_8$. Their inclusion causes the phase shift to become only a little more attractive.

The figure also shows the phase shifts obtained after the two arbitrary increases of the color confinement strength involving h.c. channels made previously for the ${}^3D_3^{NN}$ system. The phase shifts are now noticeably different from each other. Both are considerably more at-

TABLE IV: The dibaryon or resonance mass and decay width, all in MeV, in four quark models for $I = 1$ states. The channels included in the $J^P = 0^+$ state are 1c ($^1S_0^{\Delta\Delta}$ only), 2cc ($1c + ^1S_0^{NN}$), and 4cc ($2cc + ^5D_0^{\Delta\Delta} + ^5D_0^{N\Delta}$). The channels included in the $J^P = 2^+$ state are 1c ($^5S_2^{N\Delta}$ only), and 2cc ($1c + ^1D_2^{NN}$). The bound-state masses for ChQM1 are 2304 MeV for $^1S_0^{\Delta\Delta}$ and 2171 MeV for $^5S_2^{N\Delta}$ [2].

N_{ch}	ChQM2	ChQM2a	QDCSM0	QDCSM1	QDCSM3	
	M	M	M	M	M	Γ
$J^P = 0^+$:						
1c	2395	2390	2335	2231	2148	-
2cc	nr ^a	nr	nr	nr	2448	106
4cc	nr	nr	nr	nr	2433	128
$J^P = 2^+$:						
1c	ub ^b	ub	ub	ub	2167	-
2cc	nr	nr	nr	nr	2168	4

^aNo resonance in these coupled channels.

^bUnbound.

tractive than those for case 14cc, but still not attractive enough at high energies for a resonance to appear below the $\Delta\Delta$ threshold. These large changes in the low-energy phase shifts are inconsistent with experiment, thus showing that these additional h.c. effects can now be excluded.

Two other NN partial waves merit a short discussion. The 5cc $^3D_1^{NN}$ phase shifts, like their $^3S_1^{NN}$ partners, are nonresonant except for QDCSM3. All theoretical phase shifts agree well with experiment, to around 200 MeV. The quality of the theoretical $^3S_1^{NN}$ and $^3D_1^{NN}$ phase shifts shows that both quark models give good descriptions of the longer range part of the effective isoscalar central potential. The isoscalar $^5S_2^{\Delta\Delta}$ is Pauli forbidden, while the pure $^3D_2^{\Delta\Delta}$ state is unbound. As a result, the 2cc $^3D_2^{NN}$ phase shifts are nonresonant. The QDCSM values agree quite well with experiment, while the ChQMs agree less well.

B. $I=1$ states

Table IV summarizes the results for two isovector states with possible resonances. The $J^P = 0^+$ ($^1S_0^{NN}$) state is qualitatively similar to the isoscalar $J^P = 1^+$ ($^3S_1^{NN}$) state since they are mostly different spin states of the same dibaryon pairs in the same relative orbital angular momenta. The pure $^1S_0^{\Delta\Delta}$ bound state in QDCSM3 is pushed up from its unperturbed energy of 2148 MeV by 300 MeV on coupling to the $^1S_0^{NN}$ channel by the presence of a lower-mass state, the well-known slightly unbound $^1S_0^{NN}$ state. The perturbed mass is still small enough for the system to resonate below the $\Delta\Delta$ threshold.

In the remaining five quark models, the pure $\Delta\Delta$ mass is 80–250 MeV higher. In each case, the strong coupling to the NN channel pushes the state well into the $\Delta\Delta$ continuum, thus preventing a resonance from materializing. Following the procedure used for $^3S_1^{\Delta\Delta}$, the critical

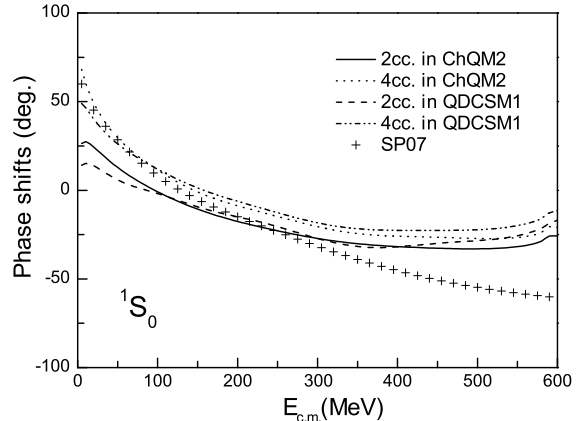


FIG. 3: NN 1S_0 phase shifts calculated with two or four coupled color-singlet channels in two different quark models ChQM2 and QDCSM1.

nucleon size below which the resonance disappears in the QDCSM is found to be $b^{\text{crit}} \approx 0.56$ fm.

Figure 3 shows the non-resonant behavior of the coupled-channel $^1S_0^{NN}$ phase shifts for ChQM2 and QDCSM1. These phase shifts become much more attractive than the experimental values from SP07 as the scattering energy increases into the resonance region, the effect being more than twice as strong as the similar behavior in the $^3S_1^{NN}$ state. All the quark models studied here do not give enough short-range repulsion in these S -states.

In the $J^P = 2^+$ state, the pure $^5S_2^{N\Delta}$ bound state appears at roughly the same mass straddling the $N\Delta$ threshold in all six quark models used. (Model differences in the $N\Delta$ S -state masses are much smaller for the high intrinsic spin state than for the low intrinsic spin states, just like the model differences in the $\Delta\Delta$ S -states.) The pure $^5S_2^{N\Delta}$ mass is pushed up only a little by coupling to the $^1D_2^{NN}$ continuum. It remains bound only in QDCSM3. The pure $^5S_2^{N\Delta}$ binding energy for ChQM1 is only 0.14 MeV. So the state is unlikely to remain below the $N\Delta$ threshold after coupling to the NN channel.

The pure $N\Delta$ state is unbound in ChQM2. (It becomes bound if the attractive central part of the scalar potential V^σ shown in Eq. (2) is increased in strength by a multiplicative factor 1.7.) The calculated non-resonant NN phase shifts are shown in Fig. 4 for ChQM2 and QDCSM1. The prominent cusp is a threshold or Wigner cusp with its maximum located right at the $N\Delta$ threshold. The phase shift above the threshold is the phase of S_{11} , where the subscript 1 denotes the NN channel. For comparison, the resonant phase shifts for QDCSM3 are also given.

Even though a resonance appears only in one quark model in our limited theoretical treatment, the masses

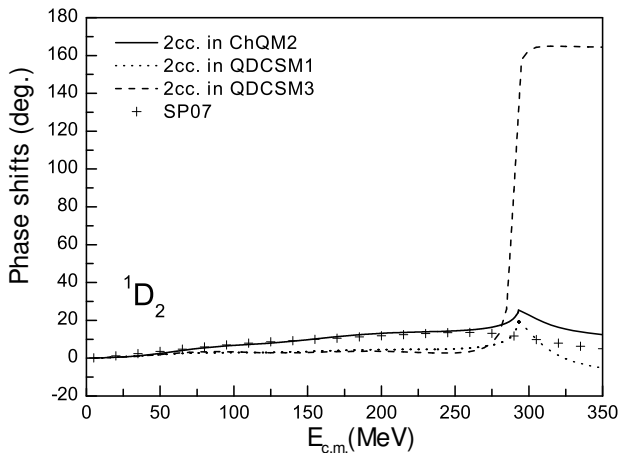


FIG. 4: NN 1D_2 phase shifts calculated with two coupled color-singlet channels in three different quark models ChQM2, QDCSM1 and QDCSM3.

involved are sufficiently close to one another and to the $N\Delta$ threshold so that they describe similar dynamical situations to within the uncertainties of the models. Moreover, the large Δ width when included would cause the state to straddle the $N\Delta$ threshold for all these quark models. We therefore consider a $^5S_2^{N\Delta}$ resonance near the $N\Delta$ threshold to be possible in all these quark models.

In fact, inelastic Argand looping (which we shall define in Sect. IV) has been obtained by Entem, Fernandez and Valcarlos [23] in the 1D_2 and possibly also 3F_3 systems for a ChQM having $\alpha_s = 0.4977$, only a little larger than the value 0.485 used in ChQM1 or ChQM2. The crucial feature in their treatment is the explicit inclusion of NN inelasticities by giving decay widths to the Δ s appearing in the coupled-channel treatment. There exist quite extensive PW solutions of both NN [16] and πd [24] scattering amplitudes in these and other isovector dibaryon systems. They could yield interesting information concerning quark dynamics in this resonance region.

We do not find any resonance attributable to an $N\Delta$ or $\Delta\Delta$ bound state in any of the quark models in the following four isovector states: (a) the $^3P_{0,1}, ^3F_3$ states (with each state calculated using three coupled color-singlet channels of the same quantum numbers for NN , $N\Delta$ and $\Delta\Delta$ constituents, respectively), and (b) the $J^P = 2^-$ state (using the four color-singlet channels 3P_2 of NN , $N\Delta$, $\Delta\Delta$, and $^7P_2^{\Delta\Delta}$).

It is worthwhile to show in Fig. 5 the difference between ChQM2 and QDCSM1 in the well-known decomposition into central, spin-orbit and tensor components of the $^3P_J^{NN}$ phase shifts:

$$\begin{aligned} ^3P_C &= \frac{1}{9} ^3P_0 + \frac{1}{3} ^3P_1 + \frac{5}{9} ^3P_2, \\ ^3P_{LS} &= -\frac{1}{6} ^3P_0 - \frac{1}{4} ^3P_1 + \frac{5}{12} ^3P_2, \\ ^3P_T &= -\frac{5}{36} ^3P_0 + \frac{5}{24} ^3P_1 - \frac{5}{72} ^3P_2. \end{aligned} \quad (7)$$

We see that the inclusion of one pion exchange (OPE)

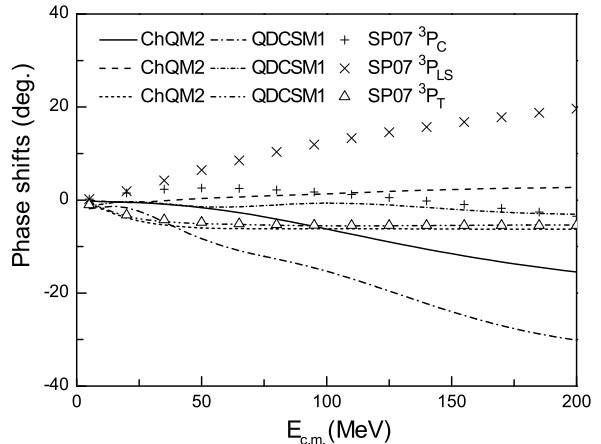


FIG. 5: The central, spin-orbit and tensor components of the $^3P_J^{NN}$ phase shifts calculated with three coupled color-singlet channels (containing NN , $N\Delta$ and $\Delta\Delta$) in two different quark models ChQM2 and QDCSM1.

takes good care of the tensor component, but both quark models give too weak spin-orbit components and too repulsive central components, especially for QDCSM1 [2, 6].

As is well known [2], the problem with the spin-orbit component comes about because the included OPE potential though clearly needed to generate a NN tensor force also contributes to the $\Delta-N$ mass difference. The color coupling constant α_s needed to account for this mass difference is then reduced to 0.3-1.0 from the value 1.7 in quark models without pion exchange. This weaker α_s gives in turn a weaker baryon-baryon spin-orbit potential from OGE. The additional spin-orbit contribution from the scalar exchange used in the ChQMs is not enough to compensate for the deficit. Resolution of this problem would require significant modifications to the quark models used.

A simple way to study the spin-orbit problem in the present limited objective of looking for dibaryon resonances without overhauling these quark models is to just modify a term or add terms to the quark-quark interaction phenomenologically. A number of related quark models are thus generated: a modified ChQM2m model, where the one gluon exchange strength α_s of the spin-orbit potential $V_{ij}^{G,LS}$ has been increased 5 times, and a number of ChQM2 ρ (f) models with the additional ρ meson exchange potential V^ρ displayed in Eq. (1). Here

$$f = \frac{\alpha_{chv}}{\alpha_{chv0}} \quad (8)$$

is the multiplicative increase of the ρ -quark-quark coupling strength above the usual and customary value $\alpha_{chv0} = 0.021$, corresponding to the coupling constant $g_{chv0} = 2.351$ used in [17]. Since the effects on these

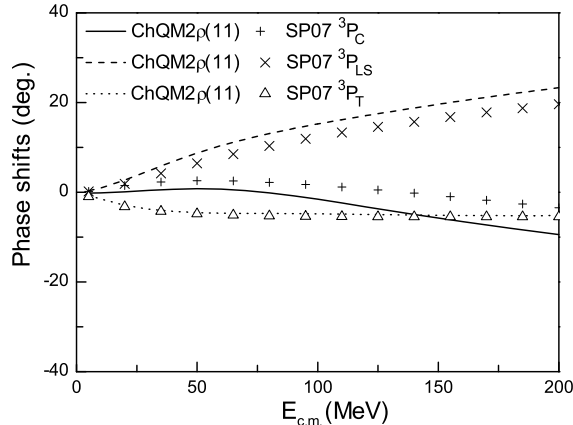


FIG. 6: The central, spin-orbit and tensor components of the ${}^3P_J^{NN}$ phase shifts calculated with only a single uncoupled NN channel in the quark model ChQM2 ρ (11).

P -wave NN phase shifts of the coupling to $N\Delta$ and $\Delta\Delta$ channels are quite small, we use only a single color-singlet NN channel to calculate the NN phase shifts for these modified models. Fig. 6 shows that the resulting central, spin-orbit and tensor components of the ${}^3P_J^{NN}$ phase shifts for the quark model ChQM2 ρ (11) give quite good agreement with the experimental SP07 values. By diagonalizing the Hamiltonian matrix in the appropriate $N\Delta$ channel, we find that none of the modified quark models described in this paragraph has a pure $N\Delta$ P -wave bound state.

The difficulty of forming P -wave bound states can readily be appreciated in the attractive square-well potential model. It is well known that to bind a P -state, its attractive potential depth must be four times that needed to bind an S -state [25]. To see how far we are from $N\Delta$ P -wave bound states for our quark models, we increase the strength of the attractive central scalar potential V^σ in ChQM2 by a multiplicative factor f_s . The ${}^3P_2^{N\Delta}$ state then becomes bound at $f_s \gtrsim 3.1$, with a binding energy of 6 (22) MeV when $f_s = 3.2$ (3.4). The potentials in the other ${}^3P_J^{N\Delta}$ states are less attractive.

A similar situation holds for ChQM2 ρ (11): Its ${}^3P_2^{N\Delta}$ (${}^5P_2^{N\Delta}$) state is unbound. It becomes bound only when its attractive central scalar potential strength has been increased by a multiplicative factor $f_s \approx 3.0$ (2.6). It is thus clear that $N\Delta$ P -wave bound states would appear only for quark models with substantially stronger attraction than those studied here.

Concerning the missing P -wave attraction in both ChQM2 and QDCSM1, one cannot just use the isoscalar scalar δ meson of mass 980 MeV that appears in the Bonn potentials [26] because of the cutoff mass $\Lambda \approx 830$ MeV used in our chiral quark models. It is not a trivial problem to reconcile these two classes of models for nuclear

forces.

Turning now to our experimental knowledge of possible resonances in NN P -states, we recall that in the PW analysis FA91 [15], resonance poles are found for the isovector odd-parity NN states 3P_2 , 3F_2 and 3F_3 . These empirical resonance-like solutions reproduce the empirical Argand loopings of the PW solutions, but many studies in the past [27] have left unresolved the question of whether these Argand loopings represent new dibaryon resonances. The difficulty centers around the observation of Brayshaw [28] that when decay channels with three or more final particles are present, Argand looping can appear in models known to have no resonance because their S -matrix has no pole. Brayshaw has given an explicit dynamical example for the case of the pp 1D_2 state coupled to $N\Delta$ and π^+d channels. The strong energy dependence that causes the Argand looping in his model comes from a logarithmic rescattering singularity in the $N\Delta \leftrightarrow \pi^+d$ transition amplitude near the $N\Delta$ threshold. The physical situation this singularity describes is the oscillation or exchange of a nucleon between the decaying Δ and the second or spectator nucleon with which it forms the bound deuteron d . In Brayshaw's model, there is no new ${}^1D_2^{pp}$ resonance near the $N\Delta$ threshold.

To complete our very brief review of resonance conditions, we should mention that recent studies of πN resonances [29, 30] have shown that the speed test can track the positions of resonance poles, if present, more reliably than the time delay criterion. (The speed test determines the resonance energy from the maximum speed of Argand looping as a function of the on-shell kinetic energy, while the time delay test locates it by maximizing the positive time delay of the scattered wave packet relative to the free wave packet.) A different kind of complication can appear in dynamical models that already have resonance poles, namely that the speed test can fail because the Argand looping does not have a solution with maximum speed [29]. This is an extension to another dynamical model (one having two coupled nonrelativistic two-body channels) of another old observation of Brayshaw that when relativistic many-body channels are present, true resonance poles can appear without any Argand looping [31].

In view of all these complications, we shall take the tentative but conservative position that a promising dibaryon resonance is one involving at least one Δ or N^* baryon that is a bound state below the dibaryon breakup threshold in the absence of a centrifugal potential when these baryons are treated as stable particles. In practice, the only excited baryon we are able to describe with some degree of confidence is the Δ . In the limited context of our quark models, we consider the ${}^1D_2^{NN}$ structure a promising dibaryon resonance, at least for some of our quark models, but not the NN P -wave Argand loopings.

TABLE V: Mass, decay widths (both in MeV) and branching ratio of theoretical baryon resonances in five quark models and comparison with partial-wave analyses of experimental data from SP07 [16] and FA91[15]. M_R for ChQM2a is estimated from the $4cc$ value and is shown within parentheses.

NN	1S_0	3S_1	1D_2	3D_3
$\Delta\Delta$	1S_0	3S_1		7S_3
$N\Delta$	5D_0	3,7D_1		3,7D_3
ChQM2:				
M_R				2393
Γ_{NN}				14
Γ_{inel}				136
B_{NN}				0.09
ChQM2a:				
M_R				(2404)
Γ_{NN}				9
Γ_{inel}				149
B_{NN}				0.06
QDCSM0:				
M_R				2400
Γ_{NN}				14
Γ_{inel}				144
B_{NN}				0.09
QDCSM1:				
M_R				2357
Γ_{NN}				14
Γ_{inel}				96
B_{NN}				0.13
α_s^{crit}	0.60	0.57		
QDCSM3:				
M_R	2433	2393	2168	2273
Γ_{NN}	130	70	4	17
Γ_{inel}	190	136	117	33
B_{NN}	0.41	0.34	0.03	0.34
SP07:				
M_R	none	none?	2148 ^a	?
Γ			118 ^a	
B_{NN}			0.29	0.26 ^b

^aPole position of FA91.

^bAt $W = 2400$ MeV.

IV. DISCUSSION

The theoretical resonance properties calculated in the last section are summarized in Table V. The first line for each dibaryon type gives the dominant PW. The PW responsible for the resonance trapping in the theory is shown in bold type. The experimental information used for the comparison is the PW solution SP07 [16] of NN scattering data. The four states are arranged in order of increasing relative orbital angular momentum ℓ_{NN} .

Each of our calculated resonances is an elastic resonance where the scattering phase shift rises sharply through $\pi/2$. The Argand plot of its complex PW amplitude

$$T = \frac{S - 1}{2i} \quad (9)$$

shows rapid counterclockwise motion on the unitarity circle. This mathematical behavior describes a physical picture where the NN system resonates or continues to “sound” due to its partial trapping into the resonance region, namely the closed channel containing one or two Δ s. Each of these elastic resonances has a finite but very small elastic (or NN) width.

The resonance properties shown in the table must be corrected for the width of a decaying Δ , leading to the appearance of pionic channels. Inelasticities cause the reduction $|S| < 1$ and the restriction of the Argand plot to the interior of the unitarity circle. We shall avoid Brayshaw’s two complications from many-body channels by considering only channels where for stable Δ s, the dibaryon system in our quark model treatment is a bound or almost bound two-body state. This restriction allows us to take the standard position that for these special states, rapid counterclockwise Argand looping is an acceptable signal of an inelastic resonance [27, 32]. In physical terms, leakage of the trapped system into pionic channels reduces the effect “heard” in the NN channel but does not eliminate it altogether. From the perspective of the quark models used here, the $I = 1$ odd-parity NN Argand structures are not promising candidates for dibaryon resonances.

We shall estimate inelasticities only at the crudest level of branching ratios, with

$$B_{NN} = \frac{\Gamma_{NN}}{\Gamma}, \quad (10)$$

where $\Gamma = \Gamma_{NN} + \Gamma_{\text{inel}}$ depends on the inelastic width Γ_{inel} caused by decaying Δ s. Close to the breakup threshold where the Δ s are almost on-shell, the inelastic width can be related approximately to the Δ width $\Gamma_{f\Delta} = 120$ MeV in free space by only accounting for the reduction in phase space available to a decaying bound Δ whose mass has been reduced to roughly $M_{b\Delta} \approx M_{f\Delta} - 0.5B$, where B is the binding energy of the dibaryon. Then [33]

$$\Gamma_{b\Delta}(M_{b\Delta}) \approx \Gamma_{f\Delta} \frac{k_b^{2\ell} \rho(M_{b\Delta})}{k_f^{2\ell} \rho(M_{f\Delta})}, \quad (11)$$

where k is the pion momentum in the rest frame of the decaying Δ , $\ell = 1$ is the pion angular momentum, and

$$\rho(M) = \pi \frac{k E_\pi E_N}{M} \quad (12)$$

is the two-body decay phase space at mass M when each decay product has c.m. energy E_i , $i = \pi, N$. We shall use this crude estimate indiscriminately even far below the breakup threshold, but the harm done is not great because most promising resonances are near the threshold.

If each decaying Δ in the dibaryon has a Breit-Wigner (BW) distribution of width $\Gamma_{b\Delta}$, the total mass of two decaying Δ s can be shown to have a BW distribution with width $2\Gamma_{b\Delta}$. Hence

$$\Gamma_{\text{inel}} \approx n_{b\Delta} \Gamma_{b\Delta}(M_{b\Delta}), \quad (13)$$

$n_{b\Delta}$ is the number of Δ s in the resonance. The results for different theoretical dibaryons are summarized in Table V. The shift in resonance masses caused by the coupling to pionic channels has not been included in these estimates.

The experimental branching ratios shown in Table V are obtained from the energy-dependent SP07 PW solution [16] at the stated resonance masses using the formula for coupled PWs

$$B_{NN} = \frac{\sigma_{el,J}}{\sigma_{tot,J}} = \frac{|T_{11}|^2 + |T_{12}|^2}{ImT_{11}}, \quad (14)$$

while $T_{12} = 0$ for an uncoupled PW. Here the subscripts i, j in T_{ij} are channel labels.

Our theoretical estimates can now be compared to the experimental results from the PW analysis of NN scattering data, in Table V. The absence in the SP07 PW solution of a resonance accessible from the $^1S_0^{NN}$ channel and its probable absence in the $^3S_1^{NN}$ give an approximate upper bound on the nucleon size of $b^{\text{crit}} \approx 0.53$ fm for the QDCSM. This upper bound causes the $^3D_3^{NN}$ resonance mass to exceed 2340 MeV, the interpolated value for the QDCSM at $b = 0.53$ fm.

The $^3D_3^{NN}$ resonance appears also in both ChQM2 and ChQM2a at around 2400 MeV, the resonance mass being not very sensitive to b . The resonance mass has not been calculated for the ChQM1, but is about 2420 MeV. NN S -wave resonances do not appear in ChQM with quadratic or linear confinement.

Table V also shows that the theoretical $^3D_3^{NN}$ branching ratio B_{NN} is smaller than the SP07 value. This means that the theoretical coupling to the trapping $\Delta\Delta$ channel is too weak. The theoretical branching ratio B_{NN} for the QDCSM3 resonance in the $^1D_2^{NN}$ state is much smaller than the SP07 value except for QDCSM3. This suggests that the theoretical coupling to the trapping $N\Delta$ channel is also too weak.

A. The ABC effect

The ABC effect, named after Abashian, Booth and Crowe [34] who first observed it, describes an enhancement above phase space of the missing-mass spectrum of the inelastic fusion reaction $pd \rightarrow ^3\text{He}X$. Subsequent experimental studies have been reviewed recently by Clement *et al.* (or WASA07) [11], who also report preliminary results for the exclusive reaction $pd \rightarrow ^3\text{He}\pi\pi$ from the WASA Collaboration, and by Bashkanov [35].

The enhancement is associated with a $\pi\pi$ invariant mass < 340 MeV, with the two pions emitted in parallel and in relative S -wave opposite in direction to the recoiling nucleus. The structure is isoscalar because it is seen in $dd \rightarrow ^4\text{He}X^0$, but not in $dp \rightarrow ^3\text{H}X^+$.

In the reaction $pd \rightarrow ^3\text{He}\pi^0\pi^0$, the differential cross section $d\sigma/dM_{\pi^0\pi^0}$ at fixed M_3 , the invariant $^3\text{He}\pi^0$ mass, has a maximum at ≈ 3080 MeV, just under the value of $2M_N + M_\Delta \approx 3100$ MeV. The cross section has a FWHM

TABLE VI: Experimental peak position (in MeV) and production cross section $\sigma_{d\pi\pi}$ (in mb) and width (in MeV) of the ABC effect compared to the estimate from the partial-wave solution SP07 of np scattering amplitudes under the assumption that the ABC effect comes from a dibaryon resonance in the specified PW at the resonance mass 2410 MeV. These estimates are described in more detail in the text.

Reaction	$np \rightarrow dX$	$np \rightarrow d\pi\pi$	$np \rightarrow np$	
Ref.	H-TA73[36]	WASA07[11]	SP07[16]	
PW			3S_1	3D_3
Peak	2460 ^a	2410	none?	?
$\sigma_{tot,J}$			3.6	3.2
$\sigma_{inel,J}$			0.41	2.3
$\sigma_{d\pi\pi,J}$	0.63	2.3	≈ 0.12	≈ 0.8
Γ	$> 220^a$	< 100	160^b	160^b

^aTheoretical calculation of [37].

^bFrom Eq.(13) at 2410 MeV.

of about $\Gamma_3 \approx 130$ MeV, the same as $\Gamma_{f\Delta}$. (These numbers are from Fig. 5-5 of [35].) Hence the pion in M_3 appears to have come from the decay of a slightly bound Δ . These features of the experimental data suggest that the ABC effect in these reactions comes from the decay of a $\Delta\Delta$ bound state. The preliminary WASA07 resonance peaks at 2410 MeV, about 50 MeV below the $\Delta\Delta$ threshold, with a width < 100 MeV. If the estimated width holds up, it would eliminate the larger values of $2\Gamma_{b\Delta} \approx 160$ MeV (from Table VI) to $2\Gamma_3 \approx 260$ MeV (from Fig. 5-5 of [35]). As pointed out by WASA07, such an outcome would disagree with the situation in the 1D_2 resonance whose width is close to the free Δ width even though the resonance straddles the $N\Delta$ breakup threshold.

The energy dependence of the production cross section $\sigma_{d\pi\pi}$ (all final pion states) has been measured. Two rough fits to different data are shown in Table VI. The recent preliminary WASA07 results [11] agree roughly with the older Heidelberg-Tel-Aviv data (H-TA73) [36]. Information can also be deduced from NN scattering. For comparison, the table gives the PW total and inelastic (or reaction) cross sections from the latest energy-dependent solution SP07 [16]. We must next estimate the fraction of σ_{inel} that goes through the $d\pi\pi$ channel.

The estimate is made by using the following two assumptions: (1) The single-pion production cross section in either J state is certainly not zero because a pion can be produced with the dibaryon left in isovector states. However, in order to maximize our estimate for $\sigma_{d\pi\pi}$, we shall ignore the contributions of all one-pion decay branches. (2) The experimental cross section $\sigma_{d\pi^+\pi^-}$ ($\sigma_{np\pi^+\pi^-}$) is known to be 0.270 (0.55) mb at $W = 2340$ MeV, and 0.33 (4.05) mb at $W = 2510$ MeV [38]. These points straddle the 2410 MeV ABC peak of WASA07 [11]. Both cross sections should increase significantly as one approaches the ABC peak from below. Above the ABC peak, the larger dibaryon breakup cross section probably reflects an increase in phase space, in-

cluding the number of other contributing states. We now assume that both cross sections at and below the the ABC peak are dominated by the same resonance in one of the two J states in the table. Using the ratio $0.27/0.55 \approx 0.5$ of these cross sections at $W = 2340$ MeV for the entire resonance, we therefore assume that $\sigma_{d\pi\pi} \approx \sigma_{\text{inel}}/3$ to get the rough and perhaps generous estimates shown in the table. Finally the estimated width for the two $\Delta\Delta$ states is that of Eq.(13) which includes the reduction in phase space for bound Δ s.

Table VI suggests that it is relatively unlikely that the ABC effect originates from a dibaryon resonance in the ${}^3S_1^{NN}$ channel. The main reason is that the NN scattering described by SP07 is highly elastic so that $\sigma_{d\pi\pi}$ is far too small. The situation for the ${}^3D_3^{NN}$ channel is more promising but not without difficulty unless the preliminary WASA07 estimate of $\sigma_{d\pi\pi}$ is reduced.

Additional information can be obtained from the energy dependence of the SP07 ${}^3D_3^{NN}$ scattering amplitude [16]. They are non-resonant at the QDCSM3 resonance mass of 2270 MeV, but they are too uncertain at the ABC peak at 2410 MeV to settle the question of an NN resonance there.

The resonance widths are also of interest, especially for the exclusive reaction that excludes contributions from three and more pions on the high-energy side of the possible resonance. The theoretical calculation of Bar-Nir, Risser and Schuster [37] is based on a one-pion exchange excitation to two Δ s followed by a pion emission from each Δ . Their calculated resonance width is close to free-space value $2\Gamma_{f\Delta} = 228$ MeV used in their calculation. Our estimated decay width shown in Table VI is much smaller but not as small as the preliminary WASA07 value. As for the branching ratio B_{NN} given in Table V, the calculated value for our quark models seems too small, but the experimental value from SP07 at 2400 MeV is not necessarily reliable.

In his study of the ABC effect, Alvarez-Ruso [39] has pointed out that the $\Delta\Delta$ contribution is greatly reduced when short range repulsive correlations are included in the NN channels. Then the cross section at $W = 2240$ MeV, some distance below the ABC peak, is found to be dominated by the $NN^*(1440)$, with both pions emitted by the decaying Roper resonance. However, at this lower energy region, the SP07 $np\,{}^3D_3$ Argand phase motion is not resonant.

Short range correlations are already included in the quark models used here. They are not the short-range repulsion from the exchange of vector mesons (specifically the isoscalar ω meson), which would reduce if not eliminate the $\Delta\Delta$ resonance. Our short range correlations come from Pauli antisymmetrization and channel coupling effects generated by overlapping clusters of quarks, including baryon excitations and hidden-color configurations that enhance rather than reduce these short-distance phenomena.

The relative importance of these explicit quark effects found in our studies also comes from the use of large

baryon clusters of quarks in all the quark models used here. The situation could be different if the baryon “bags” are small [40] and the meson clouds around them are thicker. Our calculated results for the dibaryon spectrum is sensitive to the model nucleon size used in the QDCSM, but not in the ChQM. The baryon spectrum on the other hand is quite sensitive to the model nucleon size, especially in the radial excitations. Past calculations in the ChQM [2] favors the choice near $b = 0.52$ fm. With this choice, the theoretical ${}^3D_3^{NN}$ resonance arising from the ${}^7S_3^{\Delta\Delta}$ bound state appears at about 2390 MeV in ChQM with quadratic confinement, probably at 2420 MeV with linear confinement, and at 2360 MeV for the QDCSM.

Experimental ed form factors at large momentum transfers that show the premature dominance of six-quark effects seem to favor the kind of quark models studied here over the more traditional short-range NN repulsive correlation [41]. The experimental confirmation of a $NN\,{}^3D_3$ resonance would be a dramatic demonstration of quark effects in the resonance region. Its experimental non confirmation on the other hand would point to a missing short-range repulsion in our quark models, a repulsion that is usually attributed to vector meson exchanges in traditional meson exchange models of nuclear forces.

V. CONCLUSION

We have studied resonances in NN scattering in a theoretical treatment of two baryon clusters of quarks interacting by Pauli antisymmetrization and by gluon and pion exchanges. The nucleons can resonate by changing into Δ s, but only if the resulting baryons attract each other with sufficient strength to stay below its S -wave breakup threshold. The absence of NN S -wave resonances in the SP07 partial-wave amplitudes places an approximate upper bound of $b < 0.53$ fm on the nucleon size in the QDCS quark model. This restriction in turn requires that the ${}^3D_3^{NN} + {}^7S_3^{\Delta\Delta}$ resonance mass should exceed 2340 MeV. In ChQMs, the NN system does not resonate in relative- S waves, but it has a 3D_3 resonance at 2390-2420 MeV. This 3D_3 resonance is thus a promising candidate for the explanation of the ABC structure at 2410 MeV in the production cross section of the reaction $pn \rightarrow d\pi\pi$.

The most promising isovector NN resonance candidate in our quark models appears in the ${}^1D_2^{NN}$ state and comes from a bound or almost bound ${}^5S_2^{\Delta\Delta}$ state. None of the quark models used has bound $N\Delta$ P -states that might generate odd-parity isovector resonances.

It is satisfying that these simple quark models containing only a few adjustable parameters fitting the N , Δ masses and the deuteron binding energy can yield physically interesting information about the possibility of dibaryon resonances at the much higher energies near the $\Delta\Delta$ and $N\Delta$ thresholds of NN scattering. Their success

is partly due to the fact a good part of the available collision energy in the center of mass frame has been used to excite the nucleons into one or two Δ s whose mass is fitted by the models. The system is thus effectively at much lower energies in these Δ channels. The success is also derived from the ability of these simple models to capture some essential features of the baryon-baryon interactions in different energy regimes in the many channels involved in the calculation.

The quark models used have many shortcomings. In the context of nonrelativistic models alone, a quantitative fit to NN phase shifts appears difficult without the fine tuning provided by the addition of the many meson exchange terms that appear in conventional boson-exchange potentials [26, 42]. The need to use both quarks and meson exchanges suggests that the resonance region of interest in this paper is a transition region between the traditional low-energy regime of baryons interacting via meson exchanges and the high-energy regime of quarks interacting by quantum chromodynamics.

From a more technical perspective, our theoretical description can be improved by treating the Δ s as decaying particles. It would be difficult to go beyond this improvement because explicit pion channels contain three or four bodies. In our discussion of the ABC effect, it is of considerable interest to improve upon our very rough estimate of the partial-wave $pn \rightarrow d\pi\pi$ production cross sections from NN partial-wave amplitudes. In spite of these limitations, it is clear that additional experimental knowledge and theoretical studies of NN properties in the NN resonance region near the $N\Delta$ and $\Delta\Delta$ thresholds will add significantly to our understanding of quark dynamics between baryons.

Finally we should add that the final report of the CELSIUS-WASA Collaboration on the ABC effect has now appeared [43]. The structure in the total cross section for the $pn \rightarrow d\pi^+\pi^-$ reaction centers at 2.39 GeV with a width of 90 MeV.

This work is supported by the NSFC grant 10375030, 90503011, 10435080.

-
- [1] M.J. Savage, arXiv:nucl-th/0612063v2.
- [2] A. Valcarce, H. Garcilazo, F. Fernandez, and P. Gonzalez, Rep. Prog. Phys. **68**, 965 (2005) and references therein.
- [3] Y. Fujiwara, C. Nakamoto, and Y. Suzuki, Phys. Rev. Lett. **76**, 2242 (1996).
- [4] Y.W. Yu, Z.Y. Zhang, P.N. Shen, and L.R. Dai, Phys. Rev. C **52**, 3393 (1995).
- [5] N. Kaiser, S. Grestendorfer, and W. Weise, Nucl. Phys. **A 637**, 395 (1998); E. Oset, H. Toki, M. Mizobe, and T.T. Takahashi, Prog. Theo. Phys. **103**, 351 (2000); M.M. Kaskulov and H. Clement, Phys. Rev. C **70**, 014002 (2004).
- [6] F. Wang, G.H. Wu, L.J. Teng, and T. Goldman, Phys. Rev. Lett. **69**, 2901 (1992); G.H. Wu, L.J. Teng, J.L. Ping, F. Wang, and T. Goldman, Phys. Rev. C **53**, 1161 (1996); G.H. Wu, J.L. Ping, L.J. Teng, Fan Wang, and T. Goldman, Nucl. Phys. **A 673**, 279 (2000).
- [7] L.Z. Chen, H.R. Pang, H.X. Huang, J.L. Ping, and F. Wang, Phys. Rev. C **76**, 014001 (2007).
- [8] R.L. Jaffe, Phys. Rev. Lett. **38**, 195 (1977).
- [9] R.L. Jaffe, Phys. Rep. **409**, 1 (2005), arXiv:hep-ph/0409065; F.E. Close, Int. J. Mod. Phys. A **20**, 5156 (2005), arXiv:hep-ph/0411396.
- [10] F.E. Close, arXiv:hep-ph/0706.2709.
- [11] H. Clement *et al.*, arXiv:nucl-ex/0712.4125.
- [12] Ch. Elster, K. Holinde, D. Schütte, and R. Machleidt, Phys. Rev. C **38**, 1828 (1988).
- [13] D. R. Entem, F. Fernández, and A. Valcarce, Phys. Rev. C **62**, 034002 (2000).
- [14] M. Kamimura, Supp. Prog. Theo. Phys. **62**, 236 (1977).
- [15] R.A. Arndt, L.D. Roper, R.L. Workman, and M.W. McNaughton, Phys. Rev. D **45**, 3995 (1992).
- [16] R.A. Arndt, W.J. Briscoe, I.I. Strakovsky, and R.L. Workman, Phys. Rev. C **76**, 025209 (2007).
- [17] I.R. Dai, Z.Y. Zhang, Y.W. Yu, and P. Wang, Nucl. Phys. **A 727**, 321 (2003); arXiv:nucl-th/0404004v1.
- [18] A. Valcarce, A. Buchmann, F. Fernandez, and A. Faessler, Phys. Rev. C **50**, 2246 (1994).
- [19] V.A. Babenko and N.M. Petrov, Phys. At. Nucl. **69**, 1552 (2006).
- [20] J.L. Ping, H.R. Pang, F. Wang, and T. Goldman, Phys. Rev. C **65**, 044003 (2002); X.F. Lu, J.L. Ping and F. Wang, Chin. Phys. Lett. **20**, 42 (2003).
- [21] A. Valcarce, H. Garcilazo, and F. Fernandez, Phys. Rev. C **54**, 1010 (1996).
- [22] T. Goldman, K. Maltman, G.J. Stephenson Jr., K.E. Schmidt, and F. Wang, Phys. Rev. C **39**, 1889 (1989). F. Wang, J.L. Ping, G.H. Wu, L.J. Teng, and T. Goldman, Phys. Rev. C **51**, 3411 (1995). T. Goldman, K. Maltman, G.J. Stephenson Jr., J.L. Ping, and F. Wang, Mod. Phys. Lett. A **13**, 59 (1998). J.L. Ping, F. Wang and T. Goldman, Nucl. Phys. **A 688**, 871 (2001).
- [23] D.R. Entem, F. Fernandez, and A. Valcarce, Phys. Rev. C **67**, 014001 (2003).
- [24] C.H. Oh, R.A. Arndt, I.I. Strakovsky, and R.L. Workman, Phys. Rev. C **56**, 635 (1997).
- [25] L.I. Schiff, *Quantum Mechanics*, 3rd ed. (McGrq-Hill, New York, 1968), pp. 84-88.
- [26] R. Machleidt, Adv. Nucl. Phys. **19**, 189 (1989).
- [27] M.P. Locher, M.E. Sainio, and A. Svare, in *Advances in Nuclear Physics*, v. 17, edited by J.W. Negele and E. Vogt (Plenum Press, New York-London, 1986), pp. 47-142.
- [28] D.D. Brayshaw, Phys. Rev. Lett. **37**, 1329 (1976).
- [29] N. Suzuki, T. Sato, and T.-S. H. Lee, arXiv:nucl-th/0806.2043v1.
- [30] R.L. Workman and R.A. Arndt, arXiv:nucl-th/0808.0342v2.
- [31] D.D. Brayshaw, Phys. Rev. Lett. **36**, 73 (1976).
- [32] W.H. Kloet and J.A. Tjon, Nucl. Phys. **A 392**, 271 (1983).
- [33] B. Julia-Diaz, T-S.H. Lee, A. Matsuyama, and T. Sato, Phys. Rev. C **76**, 065201 (2007).
- [34] A. Abashian, N.E. Booth and K.M. Crowe, Phys. Rev. Lett. **5**, 258 (1960); *ibid.* **7**, 35 (1961).

- [35] M. Bashkanov, Ph.D. Thesis, Univ. of Tübingen, 2006.
- [36] I. Bar-Nir *et al.*, Nucl. Phys. **B54**, 17 (1973).
- [37] I. Bar-Nir, T. Risser, and M.D. Shuster, Nucl. Phys. **B87**, 109 (1975).
- [38] A. Abdivaliev *et al.*, Nucl. Phys. **B168**, 385 (1980).
- [39] L. Alvarez-Ruso, Phys. Lett. **B452**, 207 (1999).
- [40] G.E. Brown, Prog. Part. Nucl. Phys. **8**, 147 (1982); M. Rho, *ibid.*, p.103.
- [41] C.E. Carlson, J.R. Hiller, and R.J. Holt, Ann. Rev. nucl. Part. Sci. **47**, 395 (1997).
- [42] R. Machleidt and I. Slaus, J. Phys. G **27**, R69 (2001).
- [43] M. Bashkanov *et al.*, arXiv:nucl-ex/0806.4942v1.